UNIVERSIDAD AUTÓNOMA DEL ESTADO DE MORELOS

Centro de Investigación en Dinámica Celular

Instituto de Investigación en Ciencias Básicas y Aplicadas

Structural characterization of the TATA binding protein molecular surface from eukaryotic parasites, identification of druggable binding pockets

M. C. ÁNGEL SANTIAGO

DRA. NINA PASTOR

LAB. DE DINÁMICA DE PROTEÍNAS Y ÁCIDOS NUCLEICOS.

Parasitic diseases caused by eukaryotic parasites

Global problem

Gut parasites

From other sites

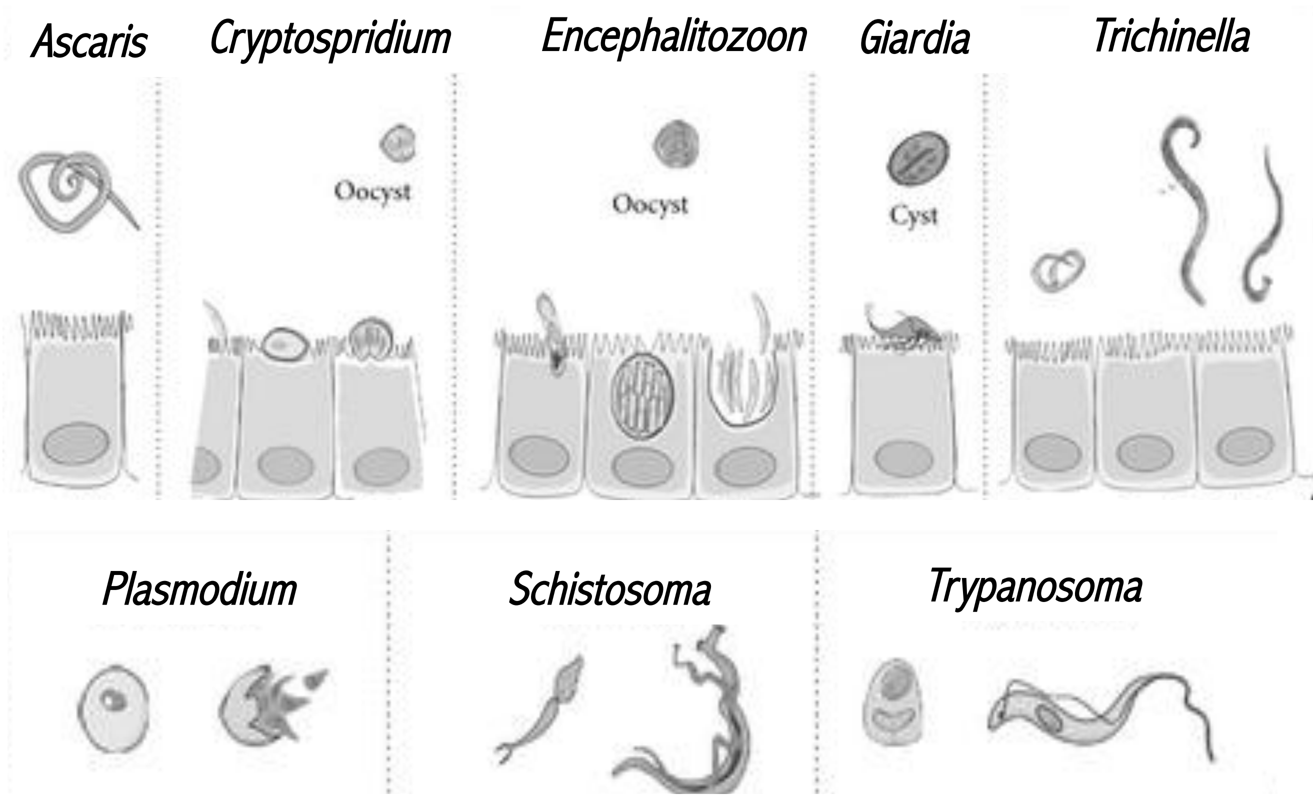

Marie Travers et al (2011), J. of Parasitology Research 2011: 610769

Antiparasitic drugs

- Drugs mainly oriented to proteins only present in the parasite
- **Drugs oriented to homologous proteins**

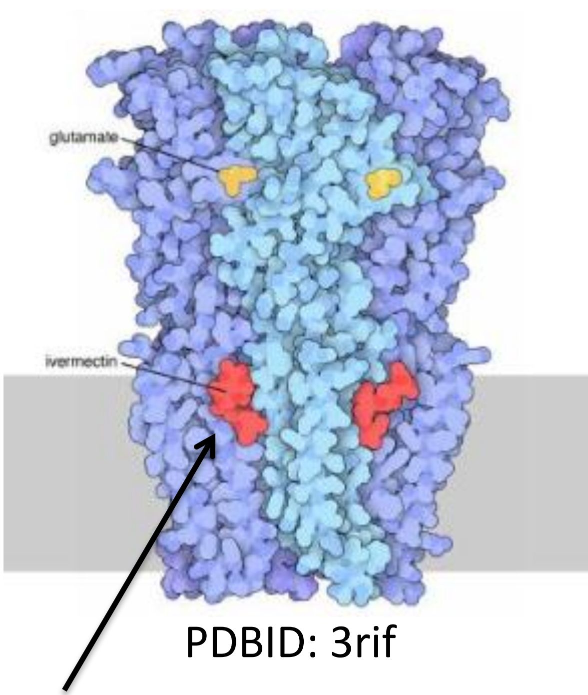

PDBID: 3rif

-**Ivermectin** (Nematodes): inhibits chloride channel → increase in ion chloride permeability.

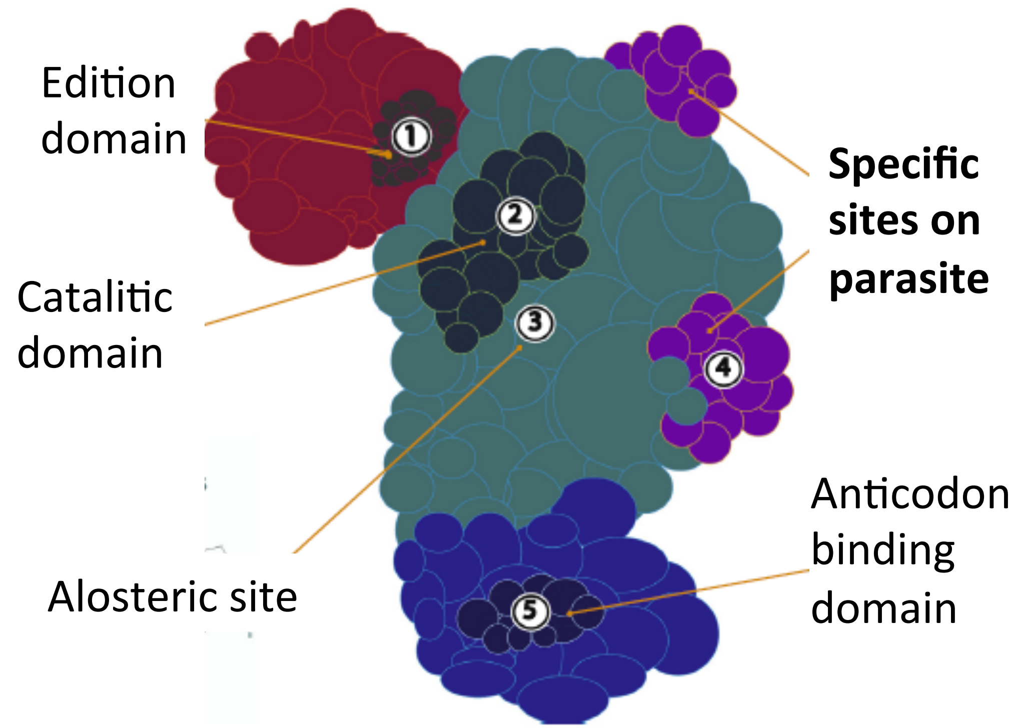

- **Benzenediol** (Plasmodium): binding to Alanine-tRNA synthetase → inhibition of parasite growth.

James S. Pham et al (2014), Int J of Parasitol Drugs Drug Resist 4: 1

TBP (TATA BINDING PROTEIN)

conserved DNA-binding domain

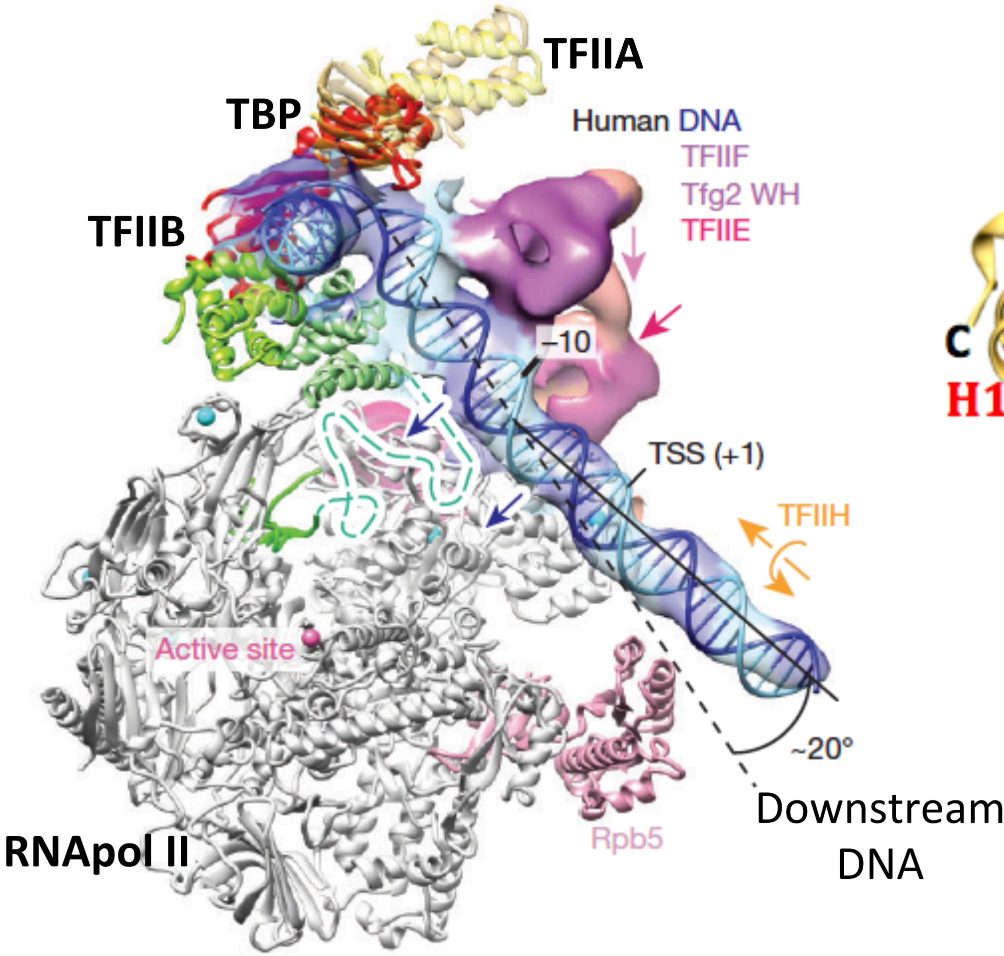

Model of the human preinitiation complex

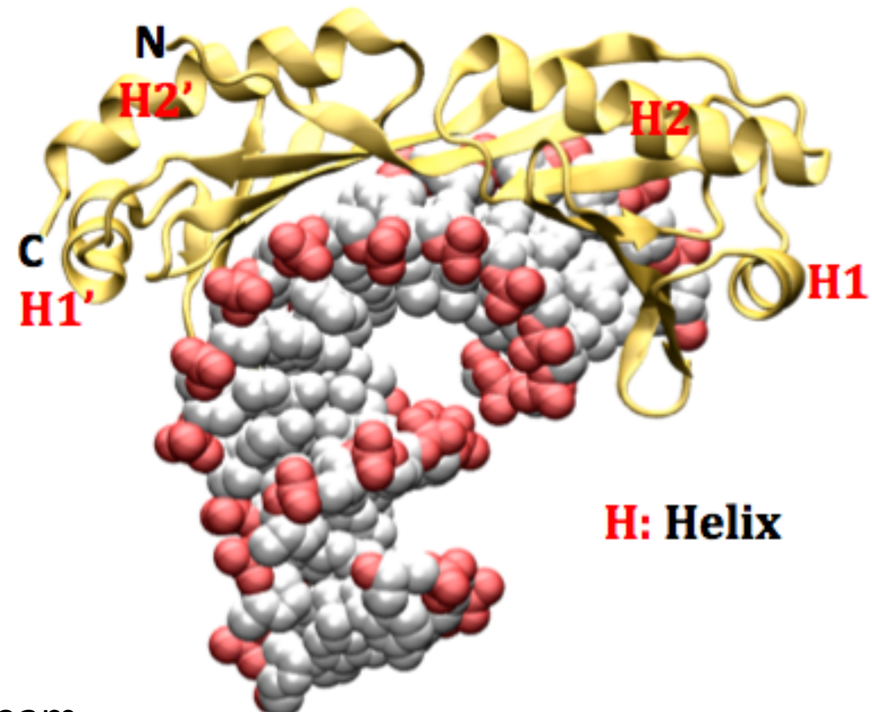

C. Plaschka et al (2016), Nature 533:353

Differences in the TBP DNA-binding domain of parasites with respect to human TBP

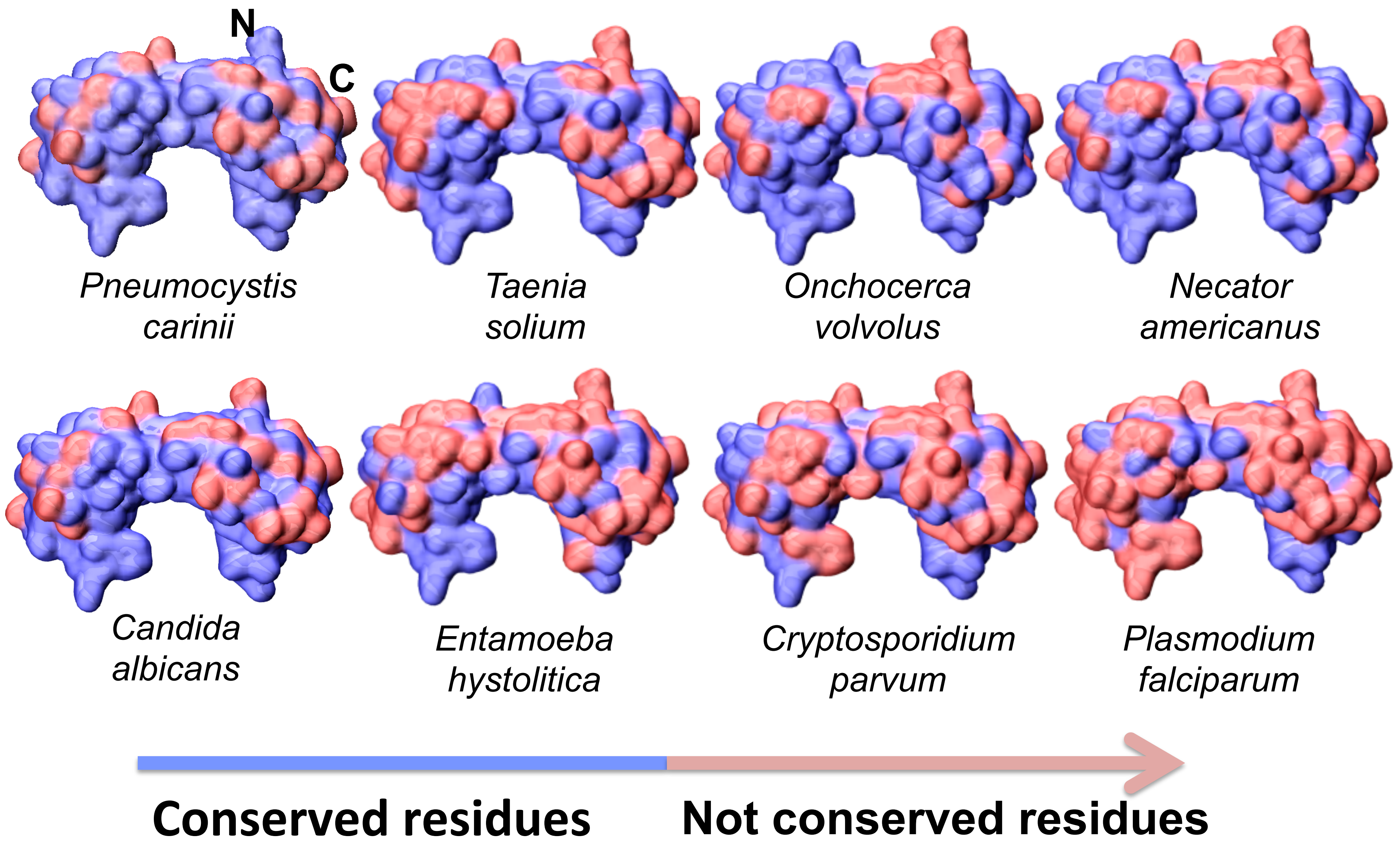

Virtual screening

Ligands
-Database: ZINC, NCI, Drug Bank.

Compounds with desired properties→ drug repurposing

Receptor
-Structure: NMR, crystal, model.
-Molecular dynamics

Structural assembly (RMSD clustering)

Screening: Docking (rigid, flexible)

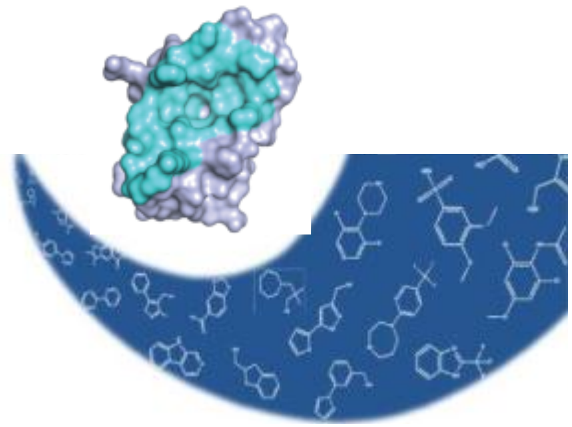

Post-docking process
-Selection of best poses (score)

Selection for experimental test

R. E. Amaro et al (2010), Med. Chem. 10:3

Receptor: Selection of TBPs

Organism	PBD code	Abreviation	Identity % with respect to human TBP	Phylum
Homo sapiens	1NVP, 1C9B, 1NGM	hsa		Mammalian
Encephatilitozoon cunniculi	3EIK, 3OC3, 4WZS	ecu	76.0	Microsporidia
Pneumocystis carinii		pnc	82.2	Ascomycota
Entamoeba histolytica		ehi	54.4	Amoebozoa
Necator americanus		nam	81.0	Nematoda
Onchocerca volvulus		ovo	82.1	Nematoda
Taenia solium		tso	76.6	Platyhelminthe
Candida albicans		cal	79.4	Ascomycota

Models generated by: I-TASSER , MODELLER, SWISS-MODEL

Y. Zhang et al (2010), *Nature Protocols*, 5:725
S. Sainsbury et. al. (2015), *Nat. Rev. Mol. Cell. Biol.* 16: 129
M. Biasini et. al. (2014) *Nucleic Acids Res.* 42:252

Modeling the flexibility of the receptor

Transient nature of the cavities on the protein surface

-main chain flexibility (large conformational changes)

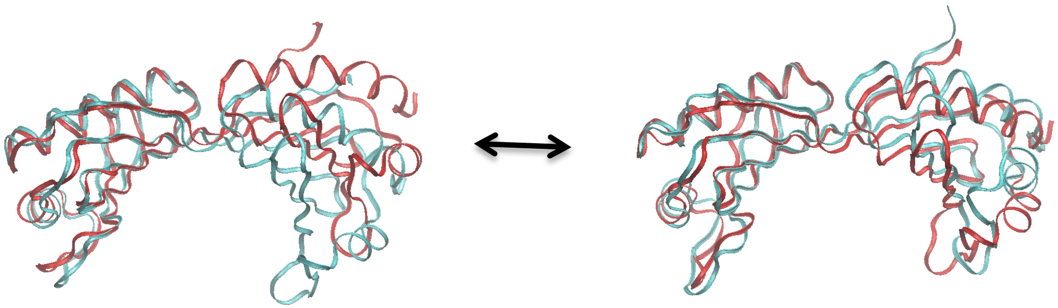

-side chain flexibility (computationally expensive during docking)

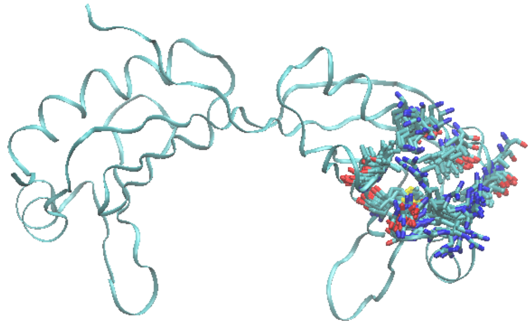

Molecular dynamics

Three runs for each TBP

100 ns.

323K → conformational sampling

Explicit solvent (TIP3), 0.15M NaCl.

NAMD, CHARMM36 potential.

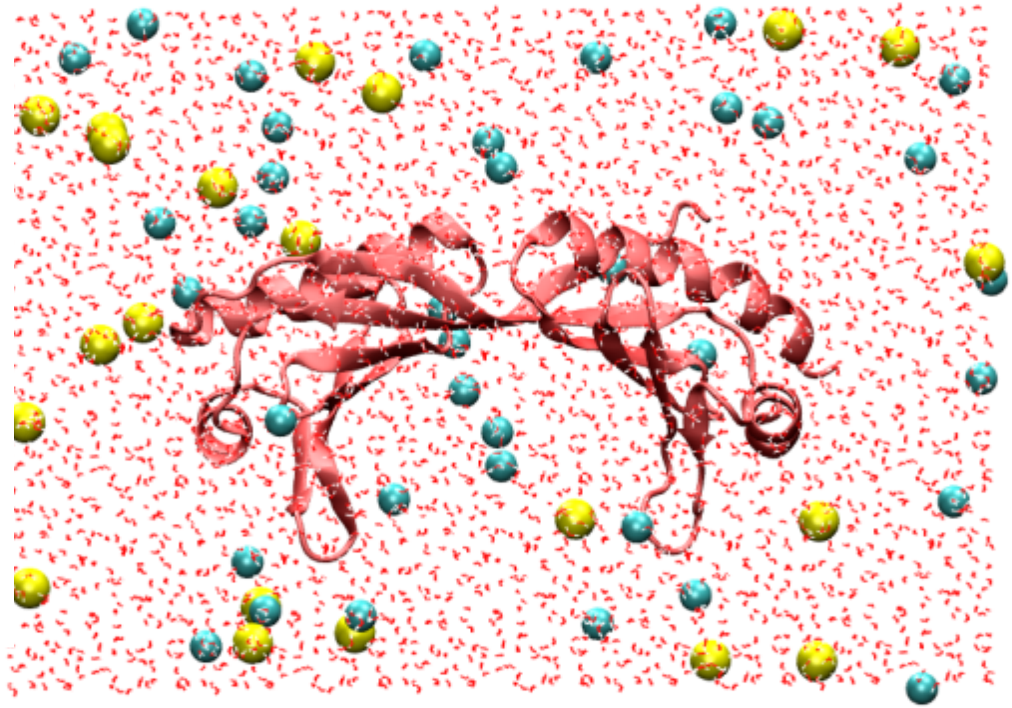

Phillips *et al.* (2005) *J. Comput Chem.* 26:1781
Brooks *et al.* (2009) *J. Comput Chem.* 30:1545

Selection of conformations for docking

2D-RMSD clustering **over main chain** (3 runs: 3000 structures)

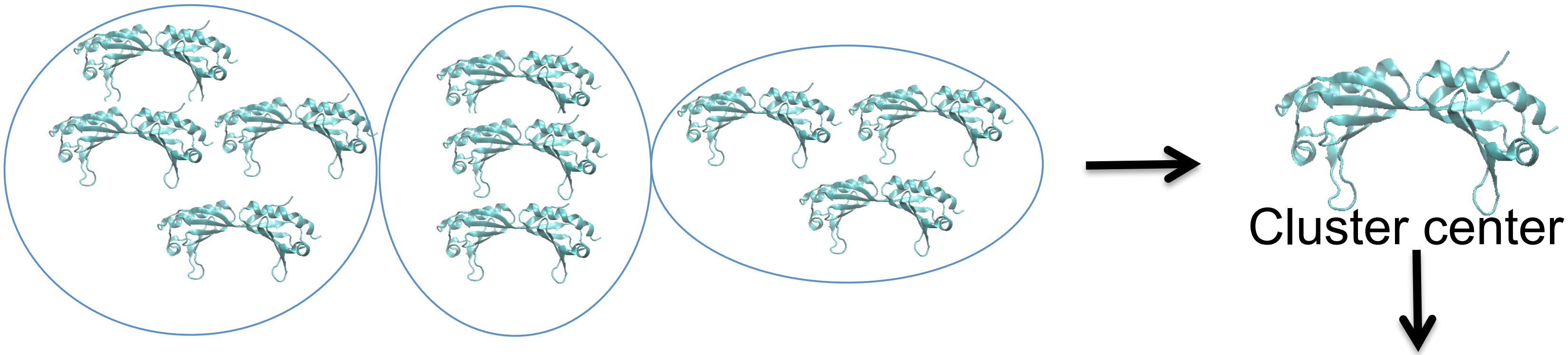

Pocket prediction with METAPOCKET

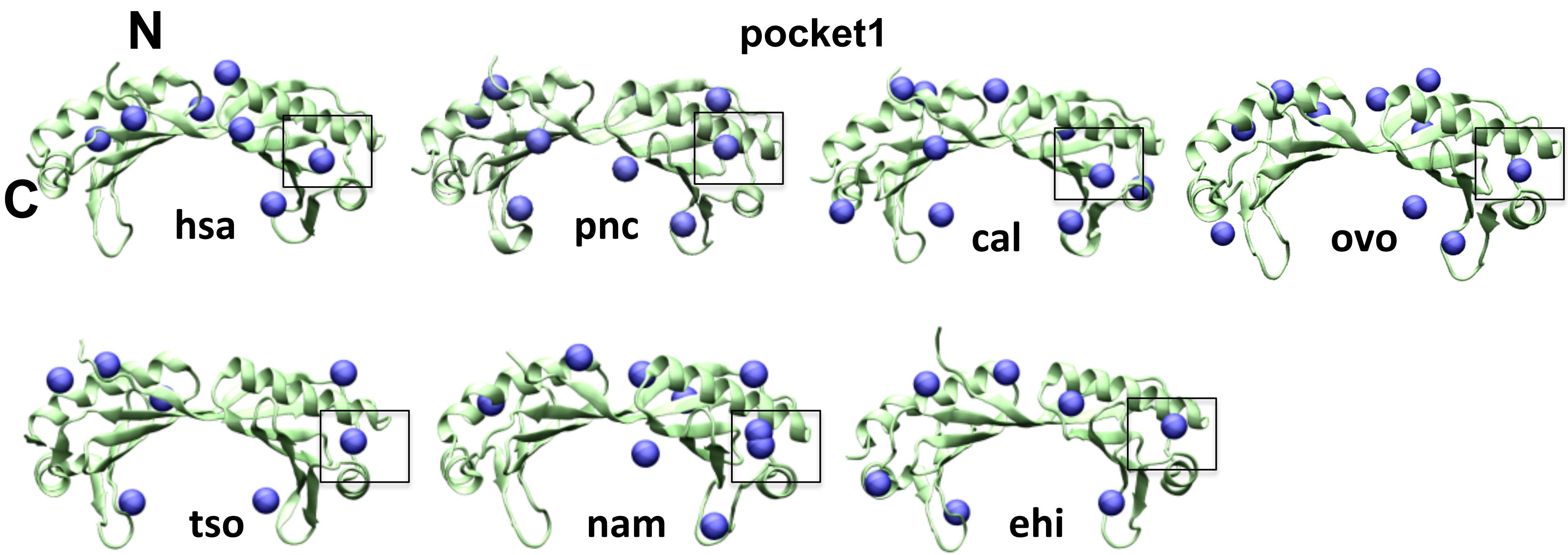

Selection of conformations for docking

Selection of residues in pocket1

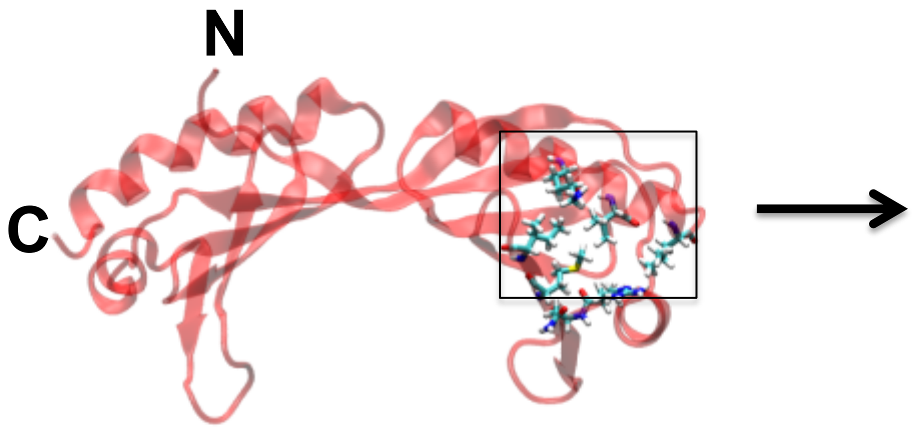

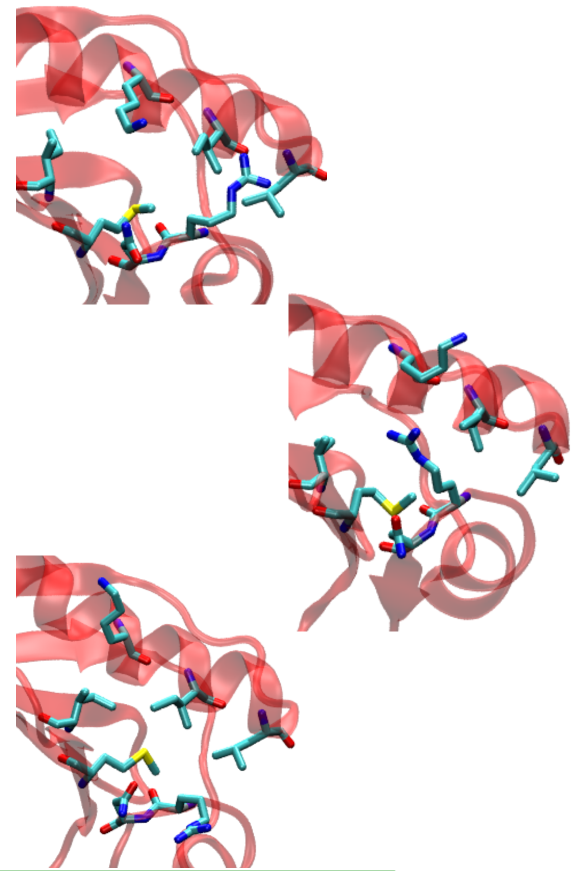

Selection of rotamer combinations of pocket residues

Selection of conformations for docking

Representative structures of the combinations

↓

Final assembly: structures with an open pocket (accesible solvent volumen > 50 Å^3)

TBP	Final assembly
hsa	10
ehi	9
pnc	12
cal	8
tso	18
nam	9
ovo	8

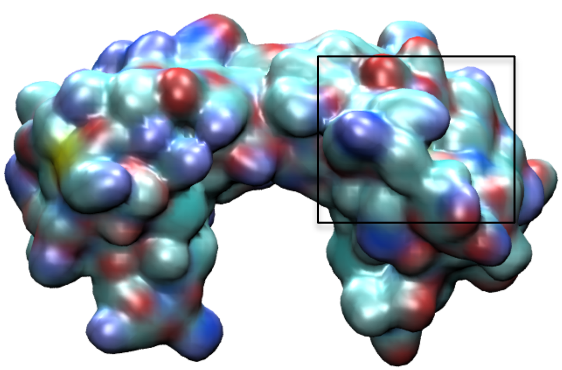

Closed pocket

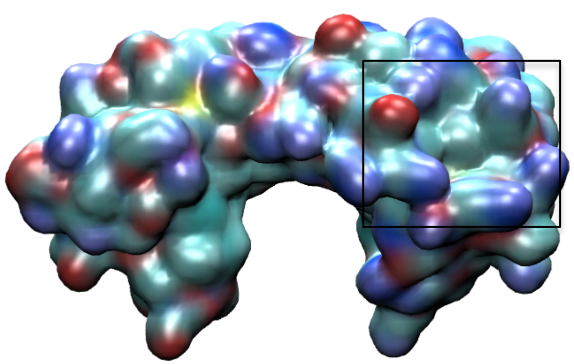

Open pocket

Selection of drug library

FDA-approved drugs obtained from ZINC database

↓

*Benign function
*Neutral compounds
*M. W. 160-500 g/mol
*LogP 0-5
*Rotable bonds ≤ 7
*Polar area ≤ 140 $Å^2$
*Donors H ≤ 5
*Aceptors ≤ 10

Drugs with higher oral bioavailability.

↓

1237 ligands

C. A Lipinski et al (2001) Advanced Drug Delivery Reviews 26:3
D. F. Veber et al (2002) J. Med. Chem. 45:2615

Docking

Autodock Vina

Rigid docking over all the surface → five best poses selected by ligand.

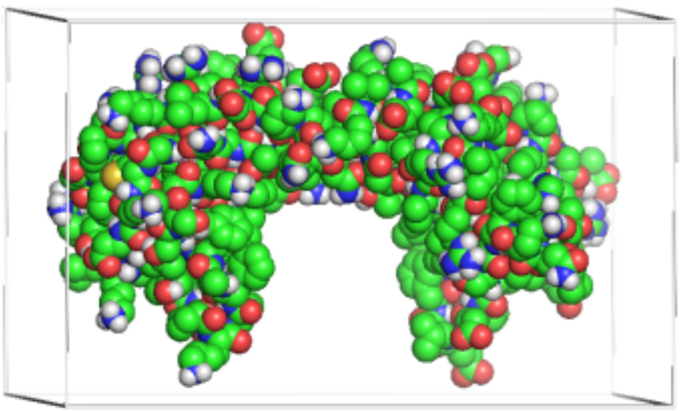

Structure assembly

Compounds around 7 Å from pocket1 residues →

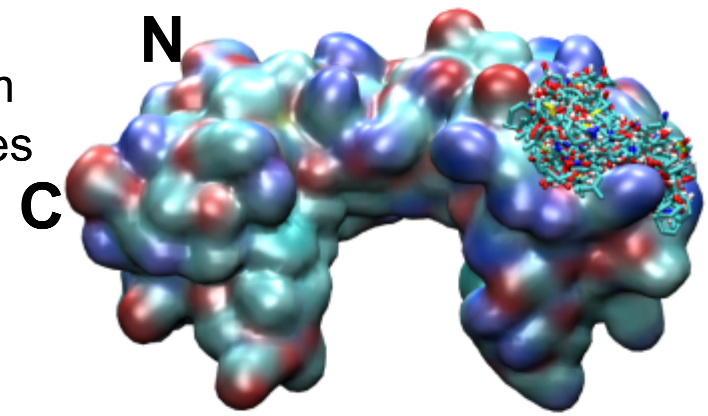

Ligands with higher binding energy to TBP of parasites.

Differences of 1.4 kcal/mol (corresponding to a ~10-fold difference in Kd's at 25 °C).

Trott O. et al (2009) J Comput Chem 31:455

Sequence differences in TBPs using ConSurf

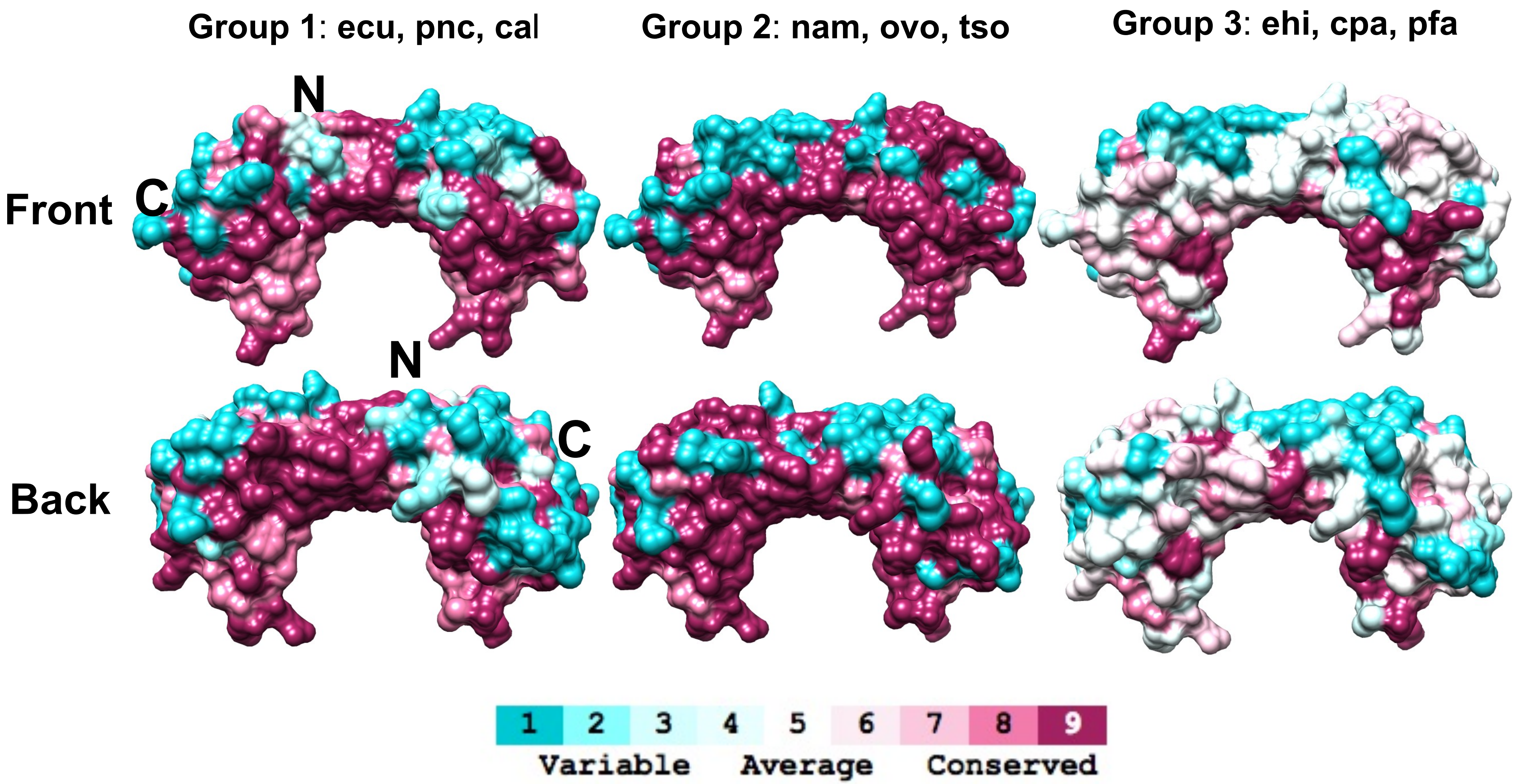

The main differences are present in the convex surface of both N and C-terminal repeats, being more marked on divergent TBPs.

H. Ashkenazy et al (2016) Nucleic Acids Research 1:408.

Electrostatic potential of human and parasitic TBPs

Pocket 1 is very conserved among these TBPs.

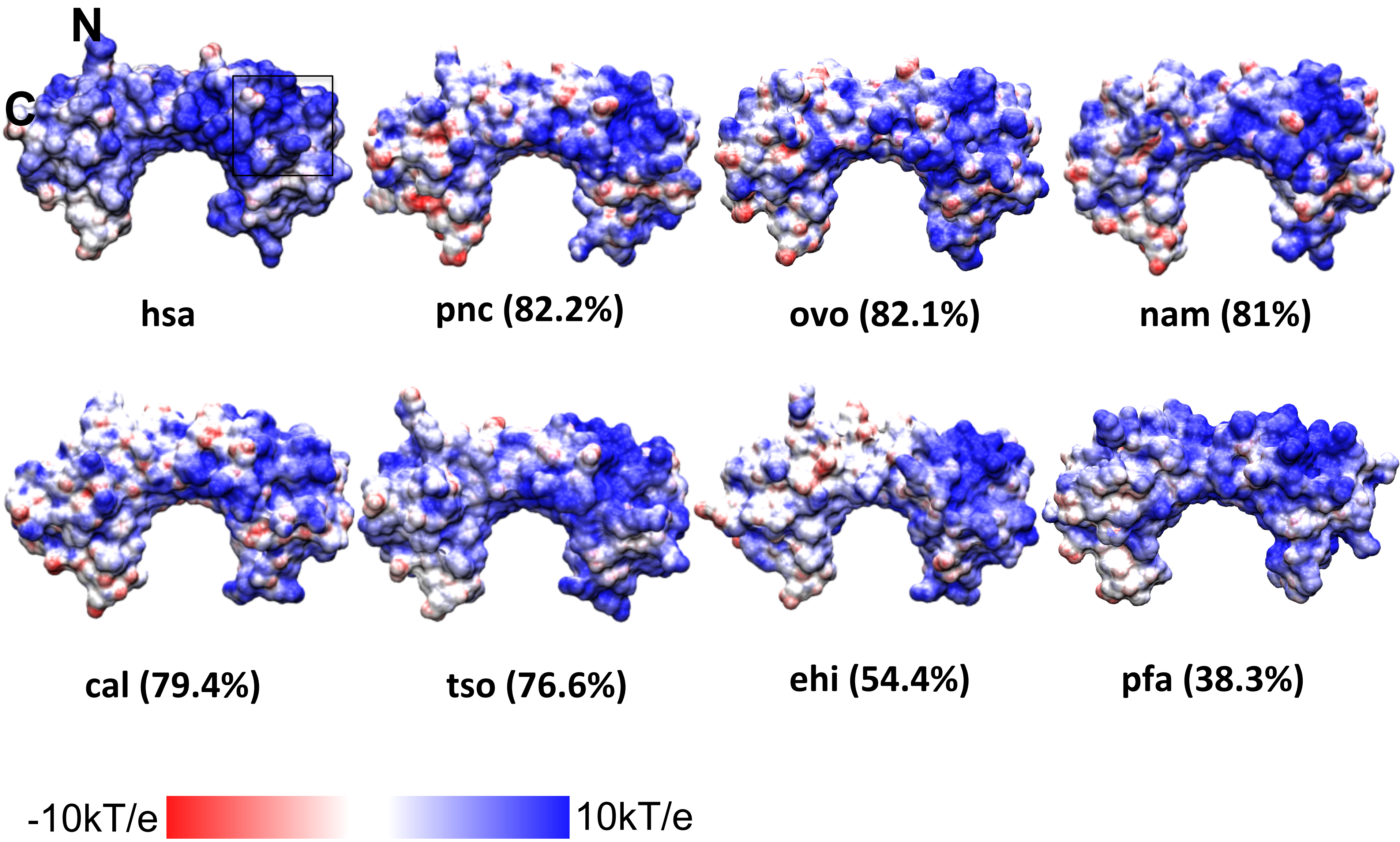

Docking

TBP	Common ligands	Energy difference between the best poses (Kcal/mol)	Binding Energy (Kcal/mol)
hsa/ehi	Norethisterone acetate Nylidrin hydrochloride	0.9 1.3	-6.8/-7.7 -4.5/-5.8
hsa/pnc	Nylidrin hydrochloride Testolactone	1.0 1.4	-4.7/-5.7 -6.5/-7.9
hsa/cal	Methohexital Norethisterone acetate	1.3 1.3	-4.8/-6.1 -6.4/-7.7
hsa/tso	Prednisone Nylidrin hydrochloride Dicumarol	1.2 1.3 1.5	-6.4/-7.6 -4.4/-5.7 -6.4/-7.9
hsa/nam	Flubendazole Sulfamethazine	1.1 1.3	-6.4/-7.5 -5.3/-6.6
hsa/ovo	Nylidrin hydrochloride Dicumarol	1.7 1.0	-4.5/-6.2

Dicumarol: anticoagulant
Testolactone: antineoplastic
Nylidrin hydrochloride: antimalarial

In the case of pnc/testolactone: binding mode with better hydrophobic interactions

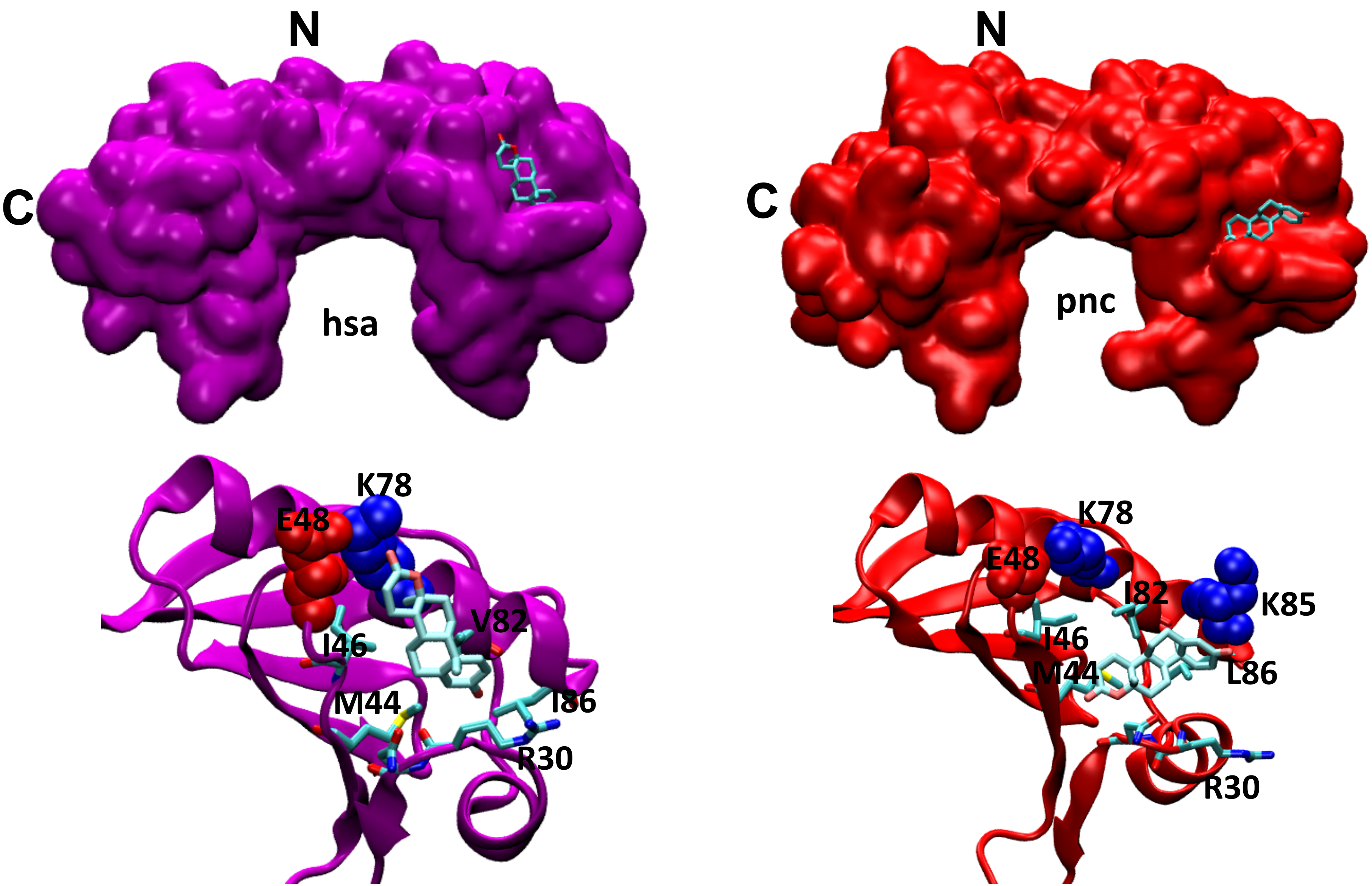

tso/dicumarol: a more open pocket1 in tso is due to the loss of a salt bridge

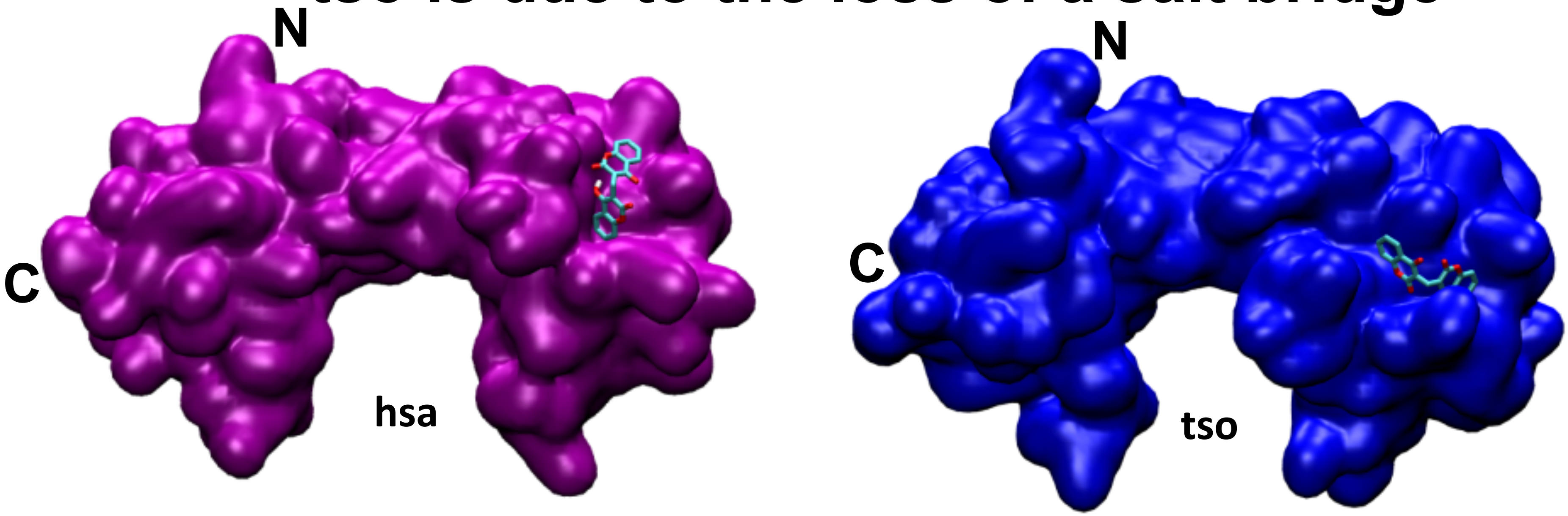

In **hsa** the salt bridge is present ~98 % of the simulation, while in **tso** only 65%.

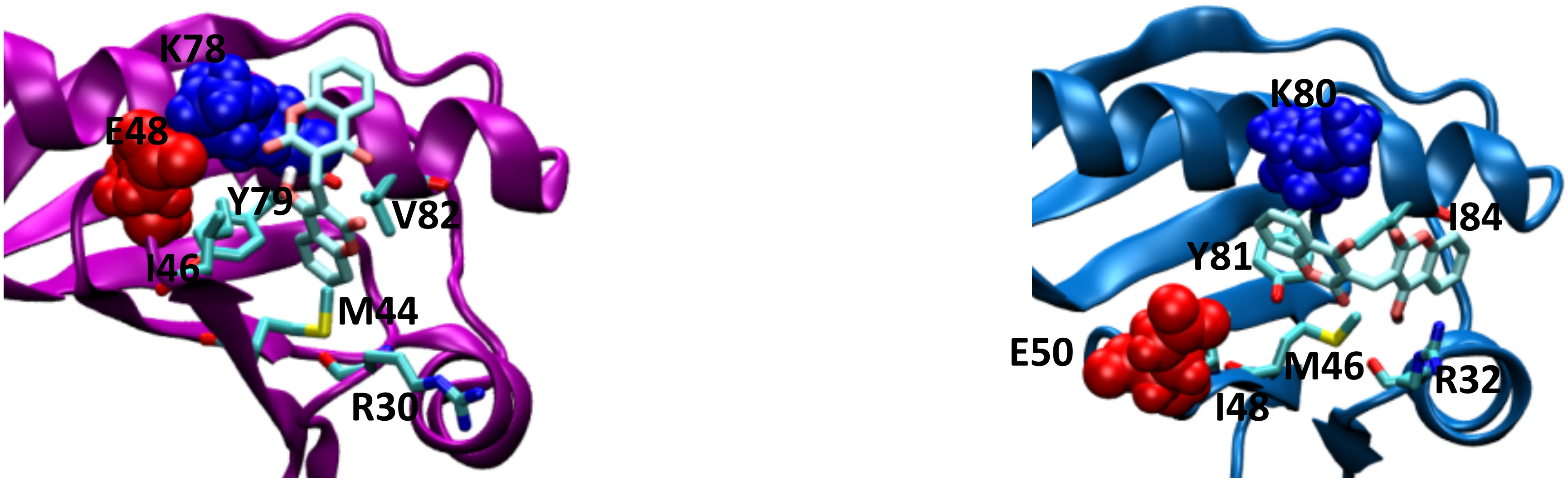

In the case of ovo/nylidrin: binding mode with an extended form promotes better interactions

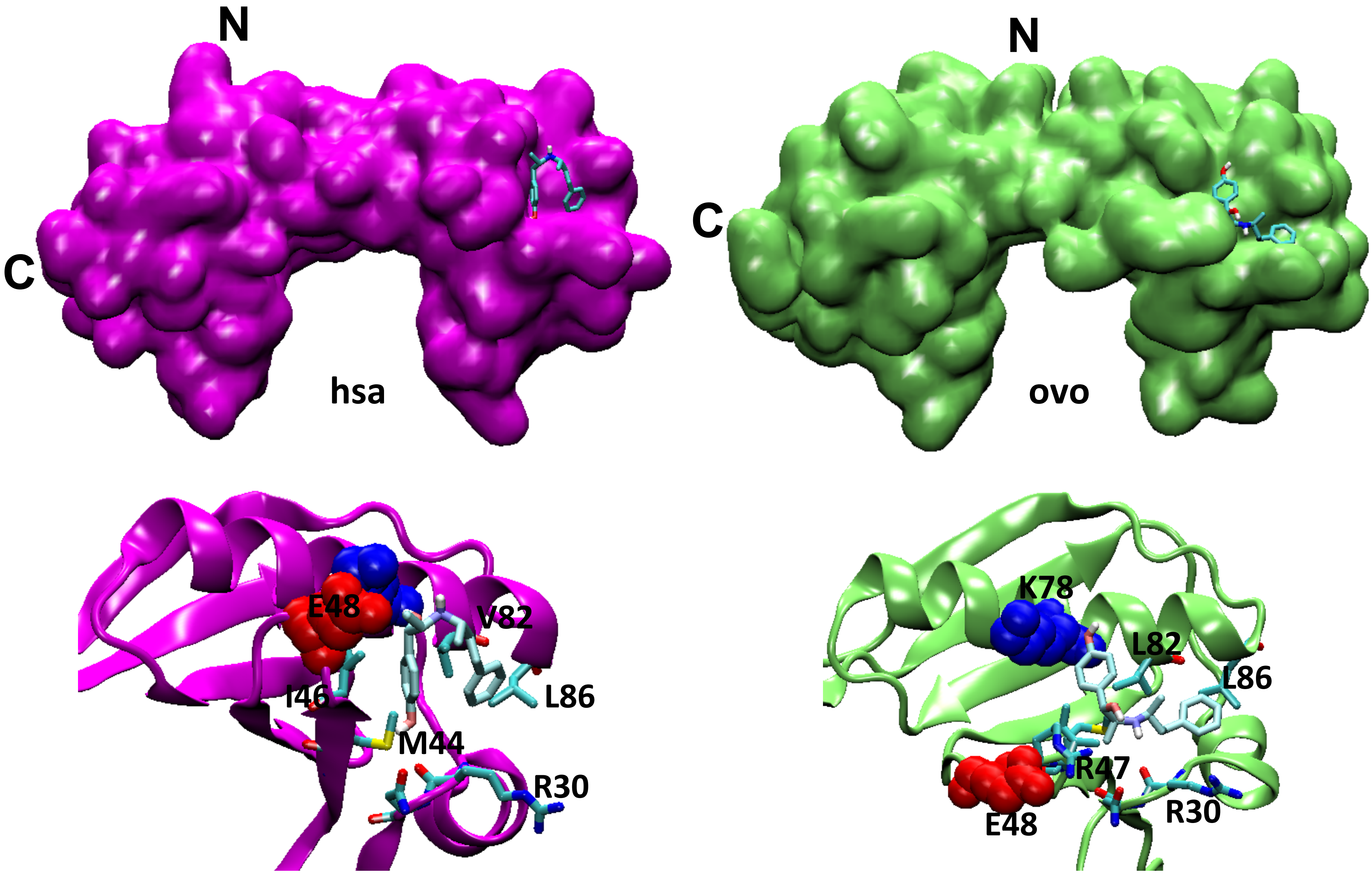

TBP interactions with other proteins

pocket1 y pocket2 : inhibition mechanism

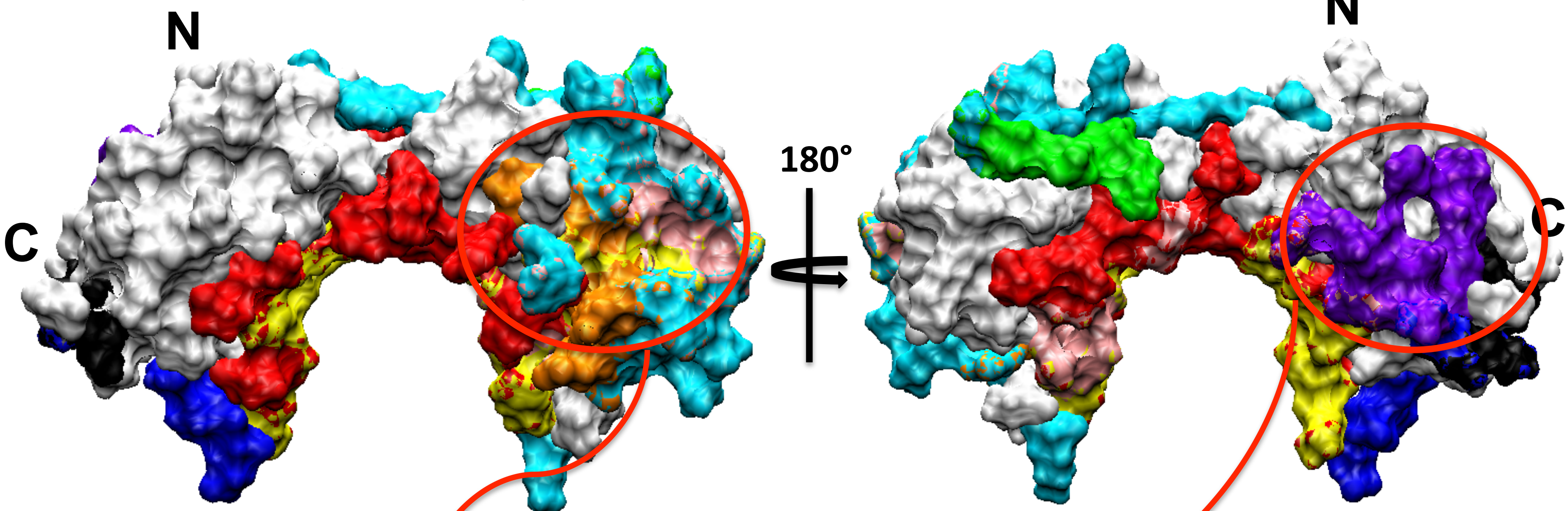

	TAF1
	MOT1
	TFIIA
	Brf1 (TFIIIB)

	NC2
	DNA
	TFIIB
	Cnd2
	Spt3 (SAGA)

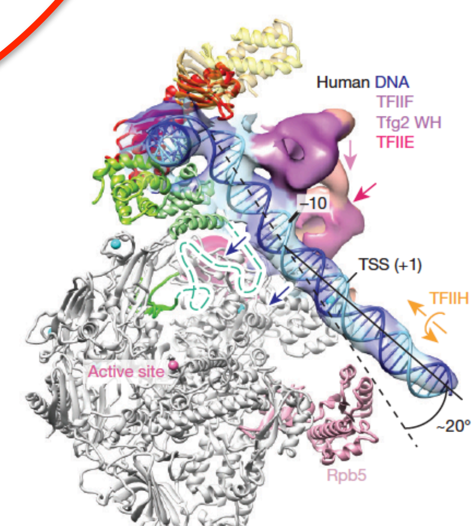

Electrostatic potential of human and parasitic TBPs

The symmetrical pocket2 is less conserved among these TBPs.

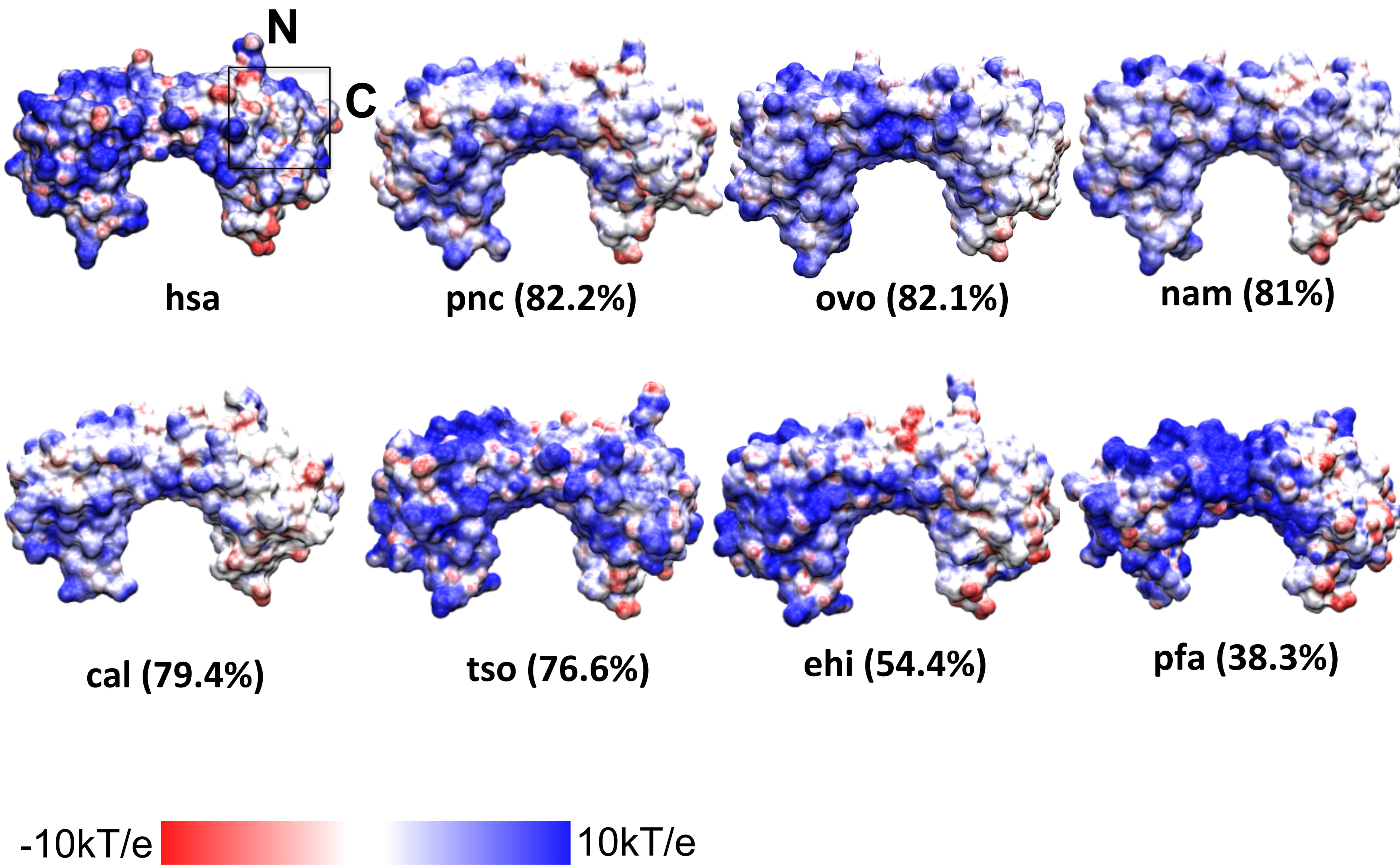

Docking

TBP	Common ligands	Energy difference between the best poses (Kcal/mol)	Binding Energy (Kcal/mol)
hsa/cal	Betamethasone	-1.5	-6.1/-7.6
	Methylprednisolone	-1.3	-6.0/-7.3
hsa/nam	Nylidrin hydrochloride	-1.4	-5.6/-7.0
	Dexamethasone	-1.2	-5.6/-6.8

Betamethasone: Corticosteroid
Nylidrin hydrochloride: antimalarial

In the case of cal/bethamesone: extended binding mode with better interactions

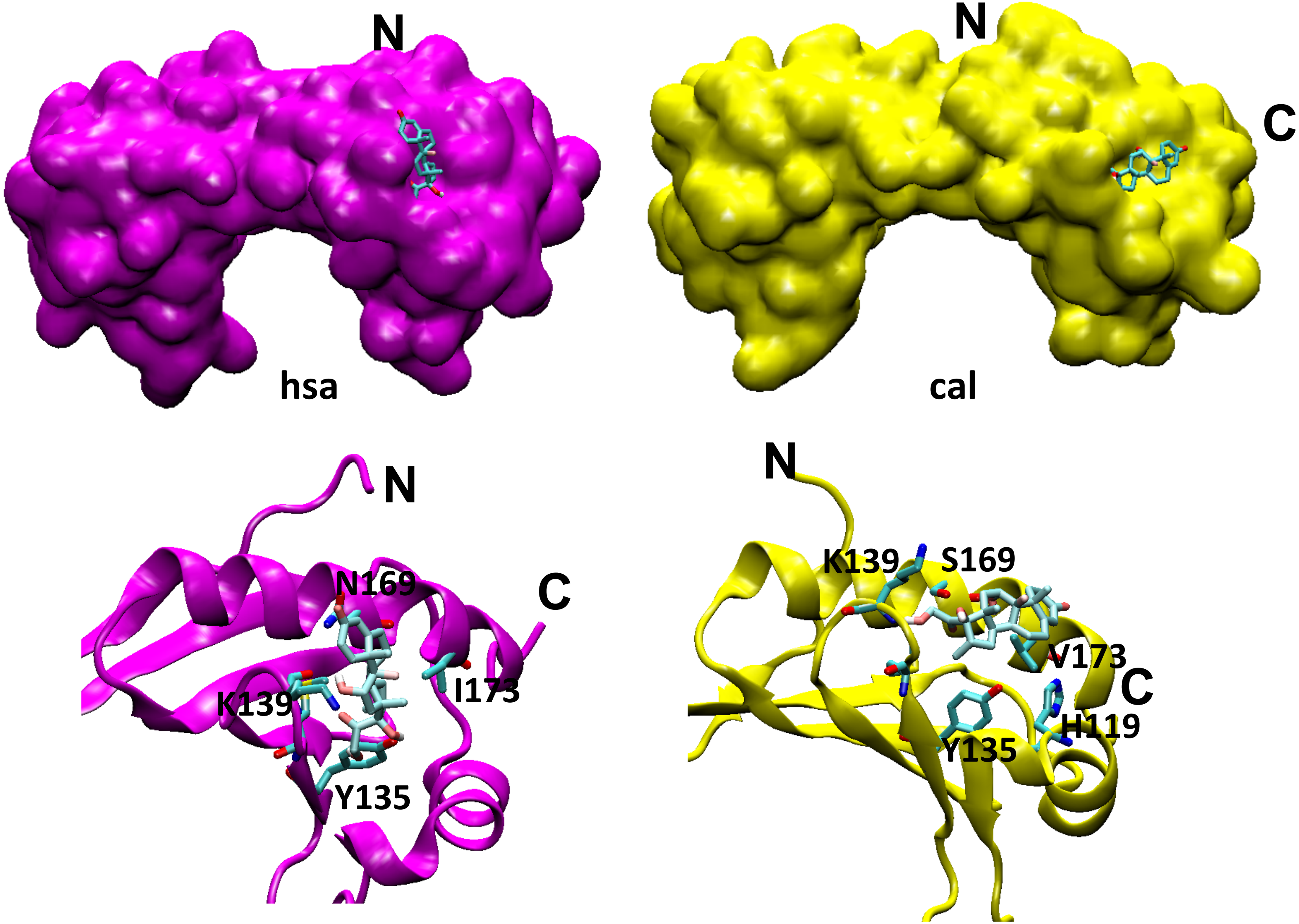

In the case of nam/nylidrin: same binding mode, but better π-π interaction with F122 and Q169

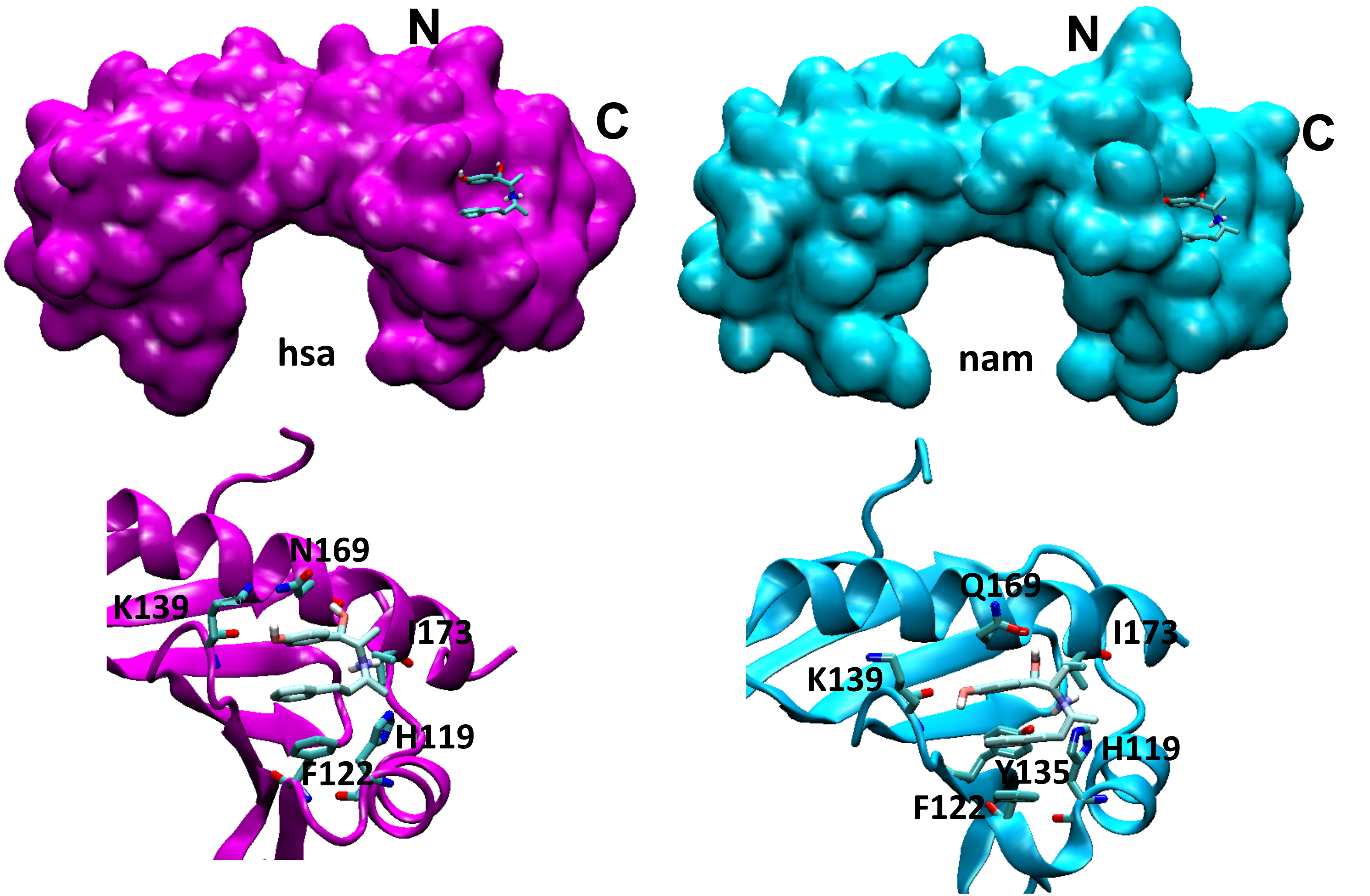

Conclusions

-The main surface differences are present in the convex part, and this is more marked in divergent TBPs.

Group 3: **ehi, cpa, pfa**

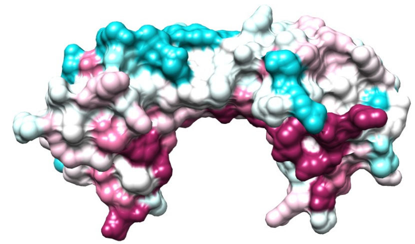

-Although the tested library showed similar binding in pocket1, we got some hits in **tso, pnc,** and **ovo** TBPs. This similar binding is due to a high conservation of pocket1.

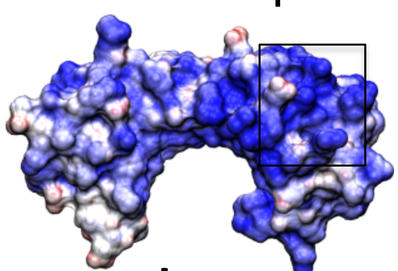

hsa

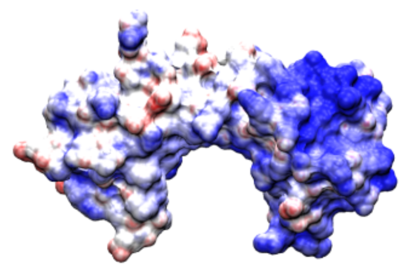

ehi (54.4%)

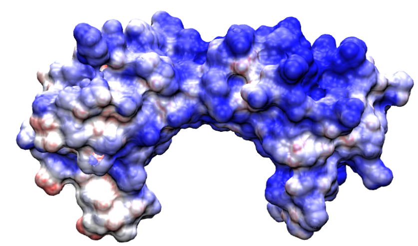

pfa (38.3%)

-The symmetrical pocket2 (binding to NC2) showed more differences in sequence and electrostatic potential distribution.

-We tested the **cal** and **pnc** TBPs in the pocket2 with the same library and we got hits for both, suggesting a potential binding pocket.

Perspectives

-More TBPs and more ligands will be tested in both pockets.

-Other pockets present in the structures remain to be analyzed and other libraries will be used (Natural products, Pubchem).

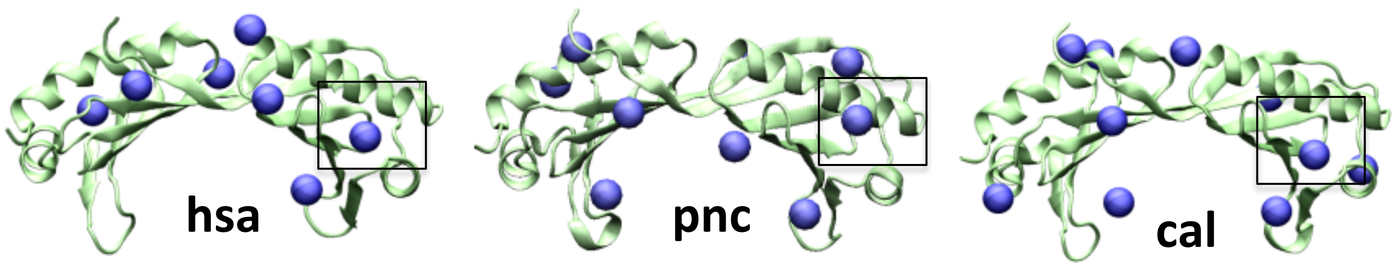

-The surfaces of TBPs like *Cryptosporidium parvum* and *Plasmodium* show more differences mainly in pocket2, and these will be tested for ligand binding.

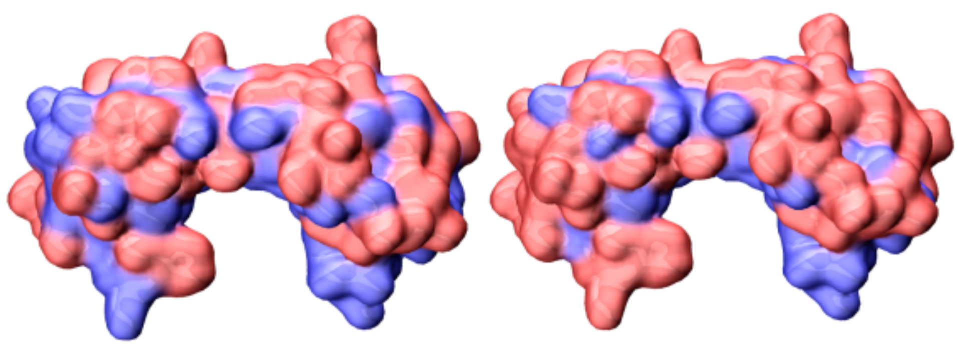

Cryptosporidium parvum   *Plasmodium falciparum*

Thanks to

Institutions

The Abdus Salam International Centre for Theoretical Physics (ICTP)

CONACYT

Centro de Investigación en Dinámica Celular

Supercomputing

UAMI — LABORATORIO DE SUPERCOMPUTO Y VISUALIZACION EN PARALELO

IPICYT — INSTITUTO POTOSINO DE INVESTIGACIÓN CIENTÍFICA Y TECNOLÓGICA, A.C.

LNS

CONACyT (PhD scholarship 292986, INFR-2014-02-231504)

Team work